Supporting Information

A large-bandgap small-molecule electron acceptor utilizing a new indacenodibenzothiophene core for organic solar cells

Pengfei Wang,[abc] Haijun Fan,[ac] Cheng Zhang[ab] and Xiaozhang Zhu,[*ab]

[a] *Beijing National Laboratory for Molecular Sciences, CAS Key Laboratory of Organic Solids, Institute of Chemistry, Chinese Academy of Sciences, Beijing 100190, China*
[b] *University of Chinese Academy of Sciences, Beijing 100049, China*

E-mail: xzzhu@iccas.ac.cn

Materials

Unless otherwise stated, starting materials were obtained from commercial suppliers without further purification. Tetrahydrofuran (THF) was dried over Na/ benzophenone and freshly distilled prior to use. Dichloromethane (DCM) was dried over CaH_2 and freshly distilled prior to use. Super dry *N*,*N*-dimethylformamide (DMF) pyridine and acetonitrile was obtained from commercial suppliers.

Measurements

Hydrogen nuclear magnetic resonance (^{1}H NMR) and carbon nuclear magnetic resonance (^{13}C NMR) spectra were measured on Bruker Avance 400, Bruker Avance III 400 HD, and Bruker Avance 600 spectrometers. Chemical shifts for hydrogens are reported in parts per million (ppm, scale) downfield from tetramethylsilane and are referenced to the residual protons in the NMR solvent ($CDCl_3$: 7.26 ppm), (CD_2Cl_2, 5.30 ppm). ^{13}C NMR spectra were recorded at 100 or 150 MHz. Chemical shifts for carbons are reported in parts per million (ppm, scale) downfield from tetramethylsilane and are referenced to the carbon resonance of the solvent ($CDCl_3$: 77.0 ppm). The data are presented as follows: chemical shift, multiplicity (s = singlet, d = doublet, t = triplet, m = multiplet and/or multiple resonances, br = broad), coupling constant in Hertz (Hz), and integration. High-resolution mass spectra were measured from Bruker solariX or Thermo Scientific Exactive mass spectrometer by

by MALDI or APCI ion source on FT or orbit mass analyzer. Elemental analyses were measured on Flash EA 1112 elemental analyzer. UV−vis spectra were recorded on a Jasco V-570 spectrometers. Cyclic voltammetry (CV) was performed on a CHI640D potentiostat in a conventional three-electrode cell configuration with glassy-carbon electrode as the working electrode, a platinum wire as the counter electrode, Ag/Ag+ as the reference electrode and calibrated with ferrocene/ferrocenium (Fc/Fc+) as an external potential marker in dry acetonitrile solution containing tetrabutylammonium phosphorus hexafluoride (n-Bu_4NPF_6, 0.1 M) as the supporting electrolyte, and the scan rate was 100 mV/s. Thermogravimetric analysis (TGA) measurement was performed on Netzsch STA 409 PC. Differential scanning calorimetry (DSC) measurement was performed on Mettler DSC822e. X-ray diffraction measurement was carried out on Panalytical Empyrean.

Solar cell fabrication and characterization

Indium tin oxide (ITO)-coated glass substrates were cleaned by ultrasonic treatment with detergent, deionized water, acetone, and ethanol for 20 min each, and were then UV/ozone treated. A thin layer of PEDOT:PSS (Clevios P VP Al 4083) was spin-coated at 3000 r.p.m. for 30 s and then baked at 150 °C for 20 min. The substrates were then transferred to a nitrogen-filled glove box. A solution of PTB7-Th and NIDBT (1:1 weight ratio, 20 mg/mL in total weight concentration) in chlorobenzene was spin-coated at different spin rates on the top of the substrate. The films were thermally annealed on a hot plate at different temperatures. After spin-coating a thin layer of PDINO at 3000 r.p.m. for 30 s on the top of the active layer, an 80 nm Al layer was deposited under a vacuum of 10^{-4} Pa. The active area of the solar cells was 3.08 mm^2 as defined by a shadow mask. For photovoltaic measurement, the J-V curve was recorded by a Precision Source/Measure Unit (B2912A, Agilent Technologies) and an AAA grade solar simulator (XES-70S1, SAN-EI Electric Co. Ltd, 7 ×7 cm^2 beam size) coupled with AM 1.5G solar spectrum filters was taken as the light source. The light power on the surface of the sample was calibrated to be 100 mW cm^{-2} in use of a standard monocrystalline silicon reference cell (SRC-1000-TC-QZ, VLSI

Standards Inc., 2 × 2 cm^2). The external quantum efficiency (EQE) was measured by a Solar Cell Spectral Response Measurement System (QE-R3011, Enlitech Co. Ltd) with the light intensity at each wavelength also calibrated by a standard single crystal Si photovoltaic cell.

SCLC mobility measurements

SCLC mobility measurements were tested in electron-only devices with the device structures of glass/Al/active layer/Al and hole-only device structure of ITO/PEDOT:PSS/active layer/Au. The mobilities were calculated by fitting the SCLC model: $J = \frac{9\varepsilon_0\varepsilon_r\mu_0 V^2}{8L^3}$, where J is the current density, ε_0 is the permittivity of the free space, ε_r is the relative permittivity of the material, μ_0 is the zero-field mobility, L is the thickness of the active layer, and V is the effective voltage in the devices.

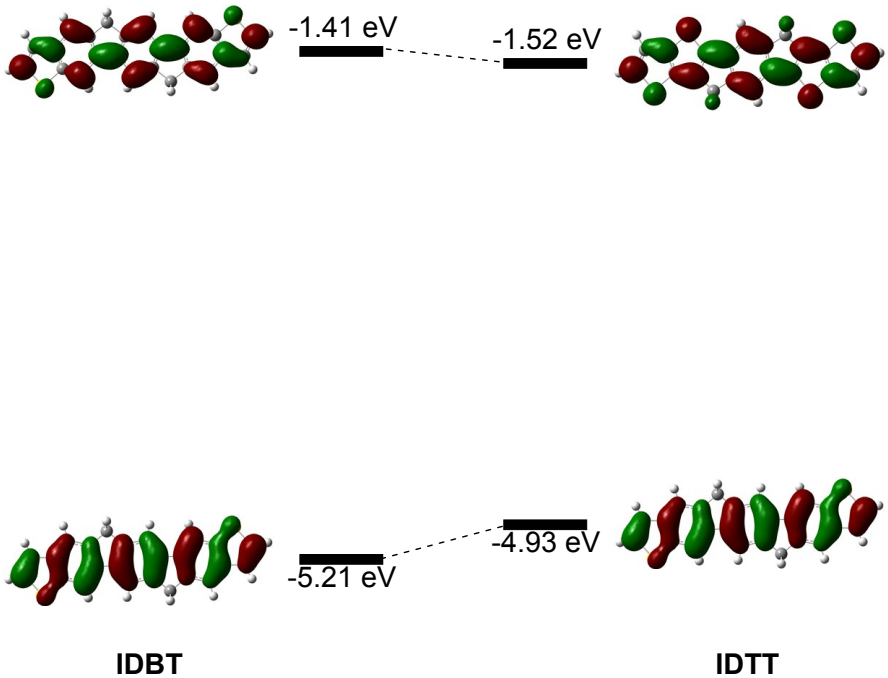

Figure S1. The frontier orbital energy level alignment of **IDBT** and IDTT (B3LYP/6-31G**).

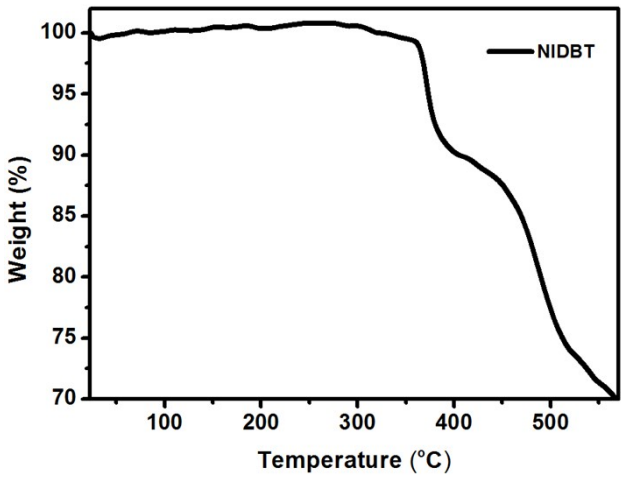

Figure S2. Thermal gravimetric analysis (TGA) curves of compound **NIDBT**.

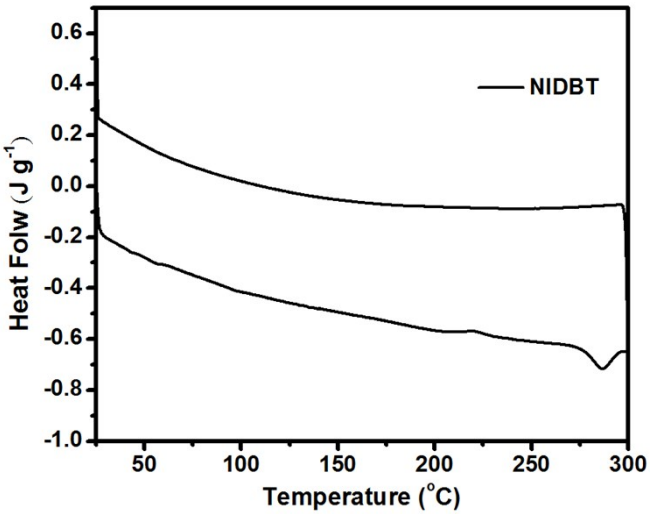

Figure S3. Differential scanning calorimetry (DSC) analysis curve of **NIDBT**.

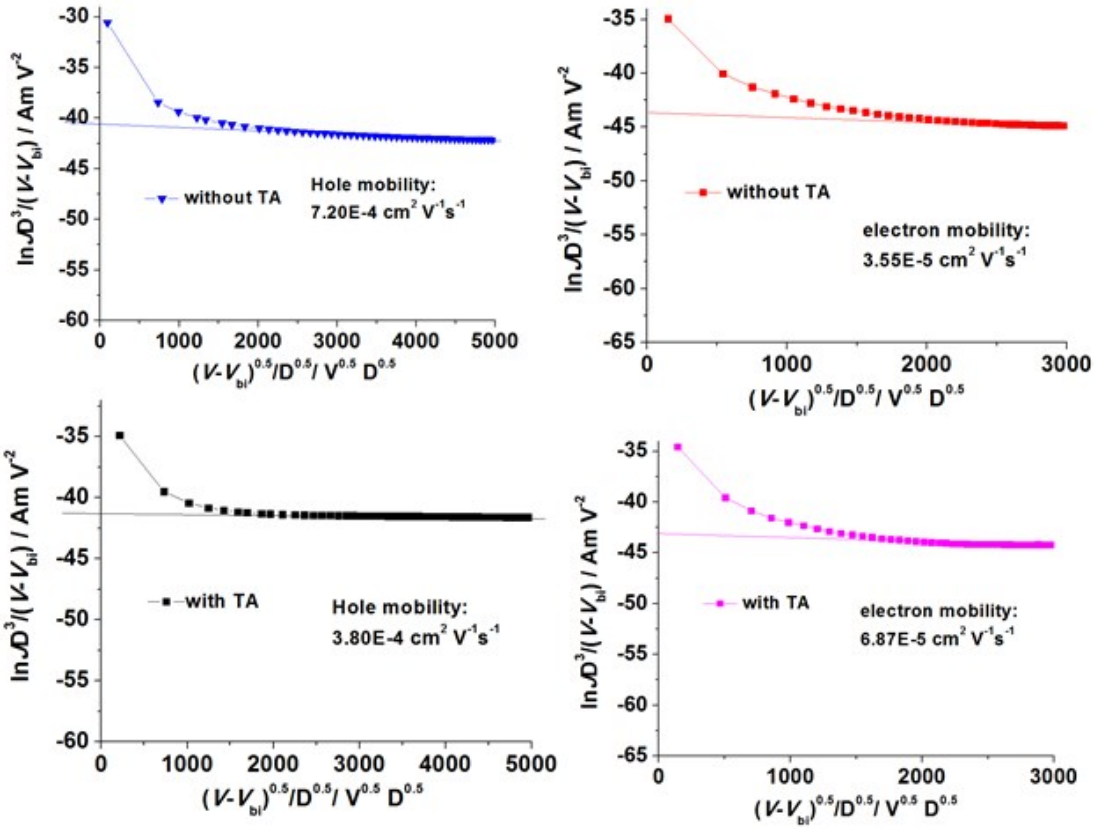

Figure S4. The SCLC curve of **NIDBT** blend film.

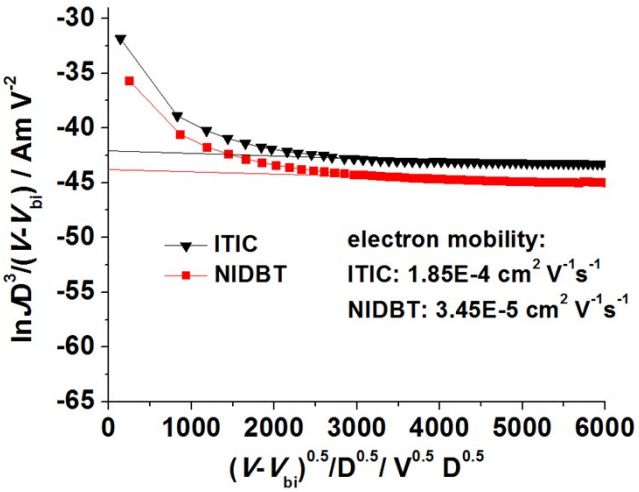

Figure S5. The SCLC curve for only electron devices with **NIDBT** and **ITIC** film.

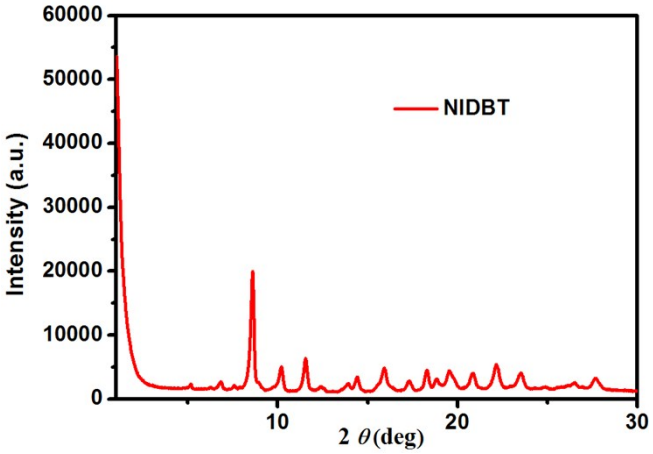

Figure S6. The X-ray diffraction (XRD) curve of **NIDBT** powder.

Table S1 Hole and electron mobility of **NIDBT**

Condition	μ_h ($\times 10^{-4}$ cm^2 V^{-1} s^{-1})	μ_e ($\times 10^{-5}$ cm^2 V^{-1} s^{-1})	μ_h/μ_e
Without TA	7.20	3.55	20.2
TA	3.80	6.87	5.53

NMR Charts

Diethyl 3,3''-dichloro-4,4''-dimethoxy-[1,1':4',1''-terphenyl]-2',5'-dicarboxylate (1)

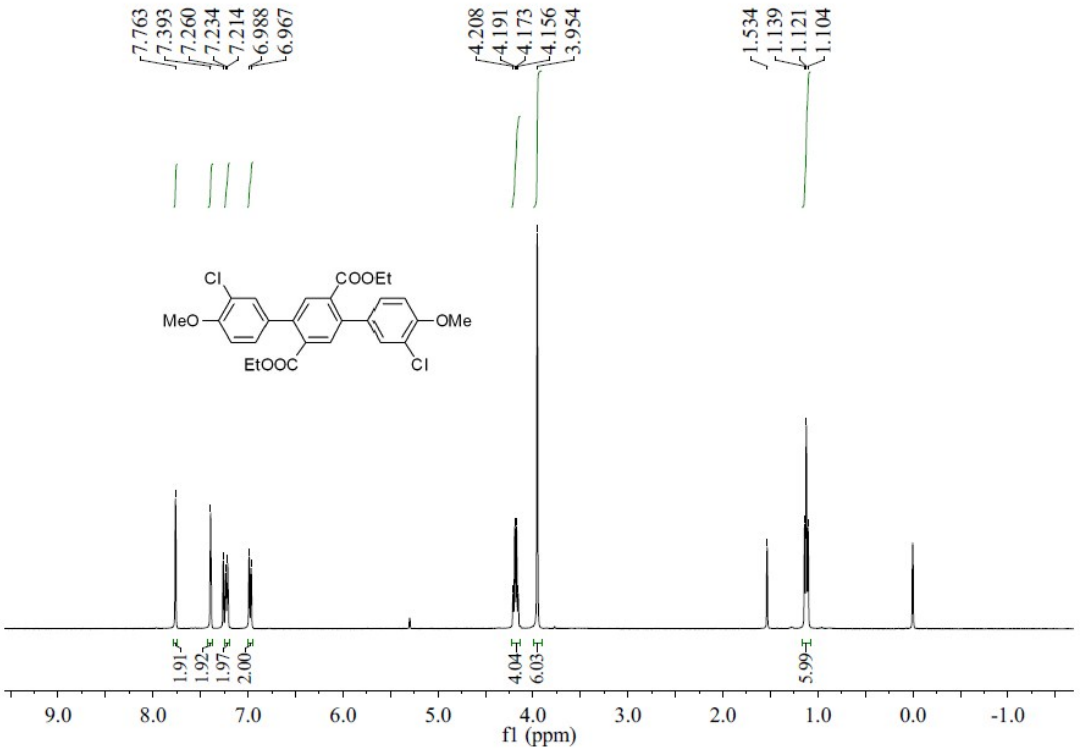

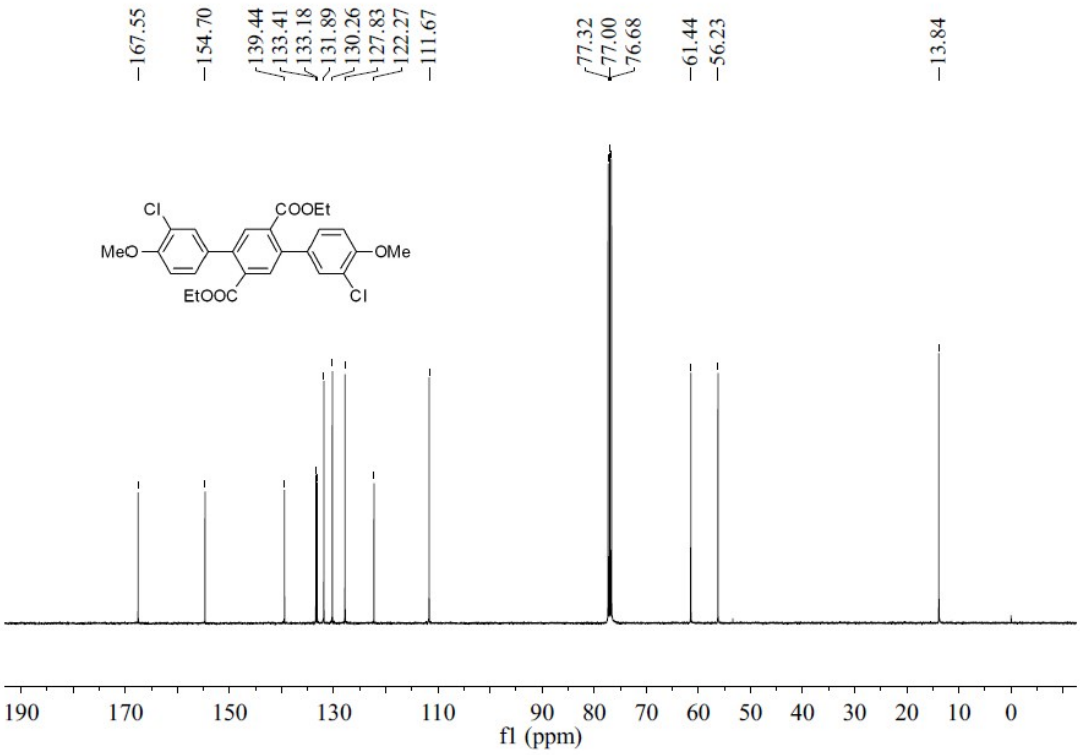

3,9-Dichloro-6,6,12,12-tetrakis(4-hexylphenyl)-2,8-dimethoxy-6,12-dihydroindeno[1,2-*b*]fluorene (2)

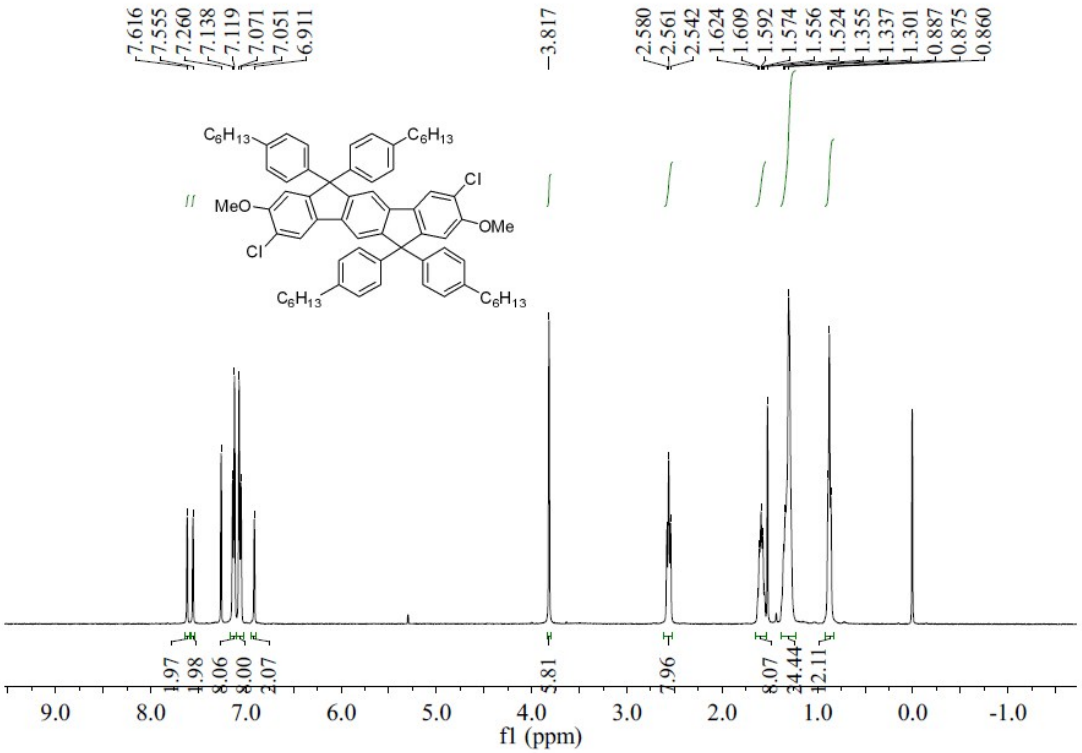

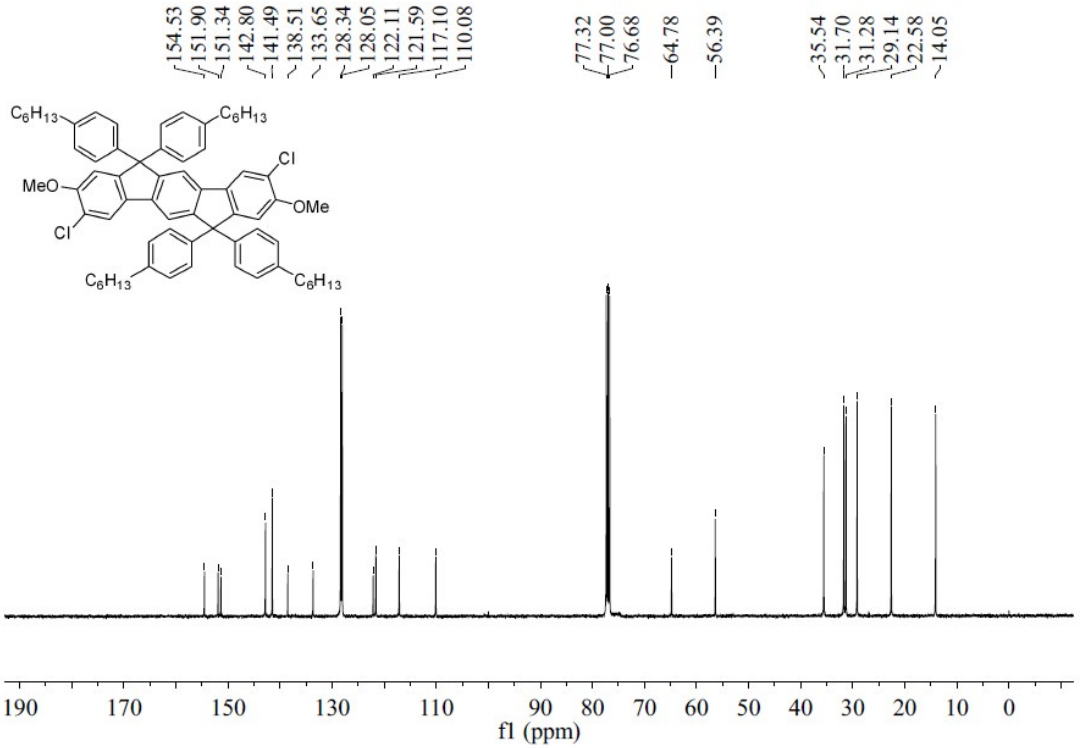

3,9-Dichloro-6,6,12,12-tetrakis(4-hexylphenyl)-6,12-dihydroindeno[1,2-*b*]fluorene-2,8-diol (3)

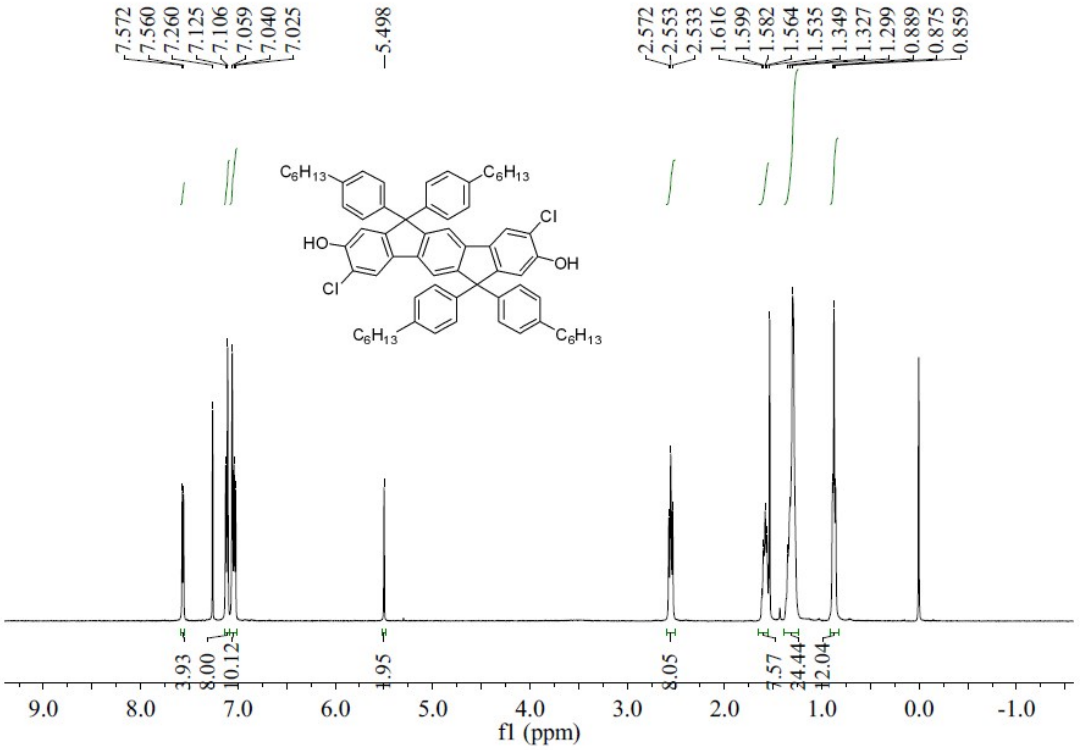

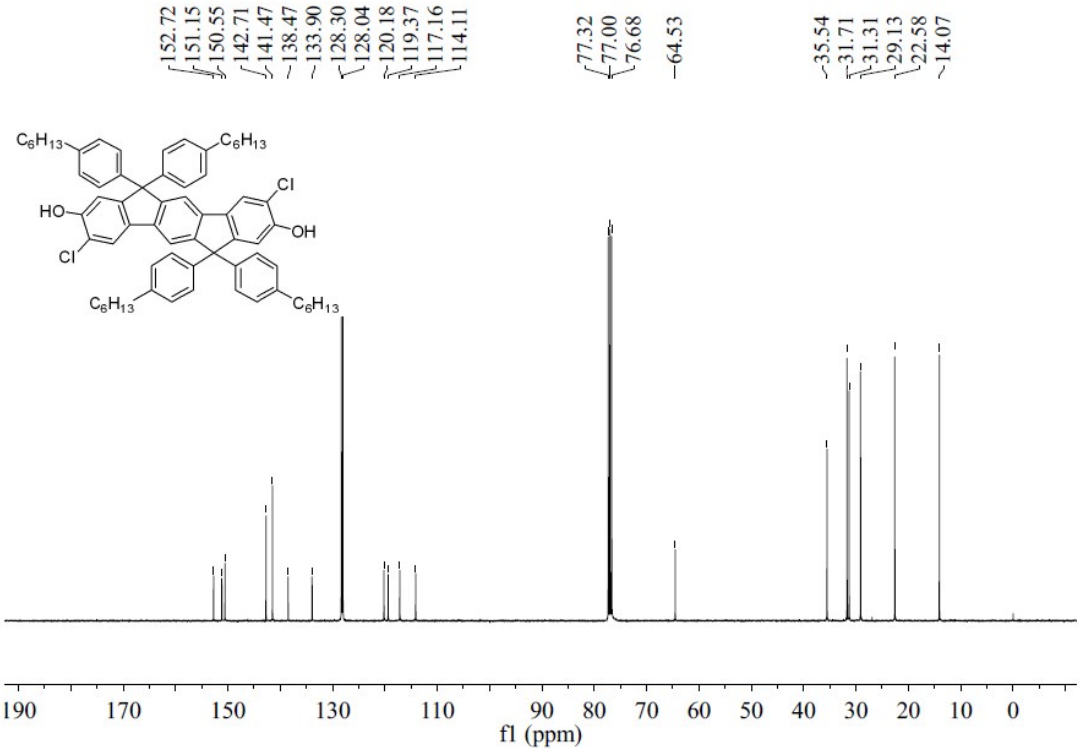

3,9-Dichloro-6,6,12,12-tetrakis(4-hexylphenyl)-6,12-dihydroindeno[1,2-*b*]fluorene-2,8-diyl bis(trifluoromethanesulfonate) (4)

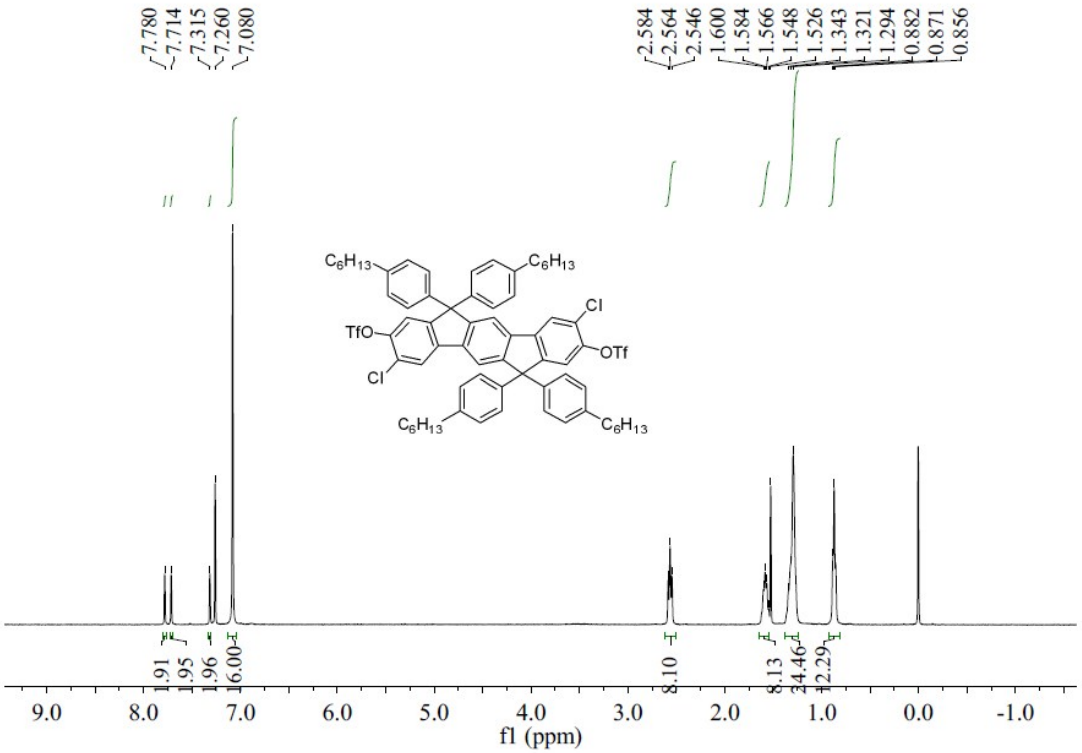

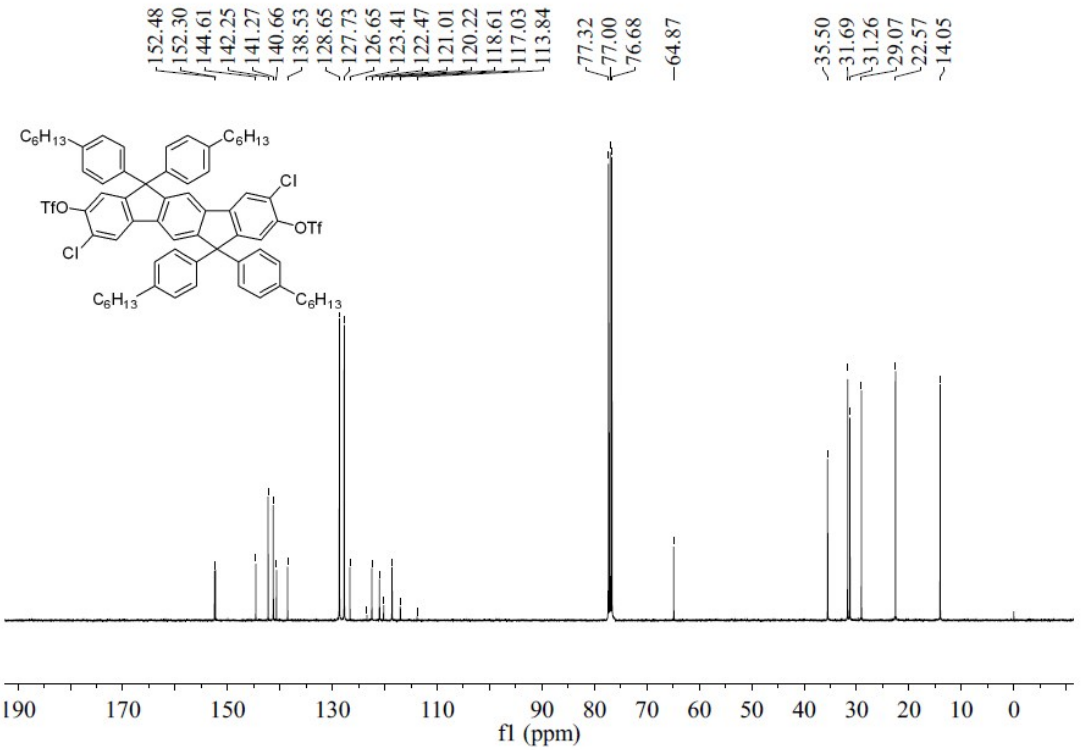

((3,9-Dichloro-6,6,12,12-tetrakis(4-hexylphenyl)-6,12-dihydroindeno[1,2-*b*]fluorene-2,8-diyl)bis(ethyne-2,1-diyl))bis(trimethylsilane) (5)

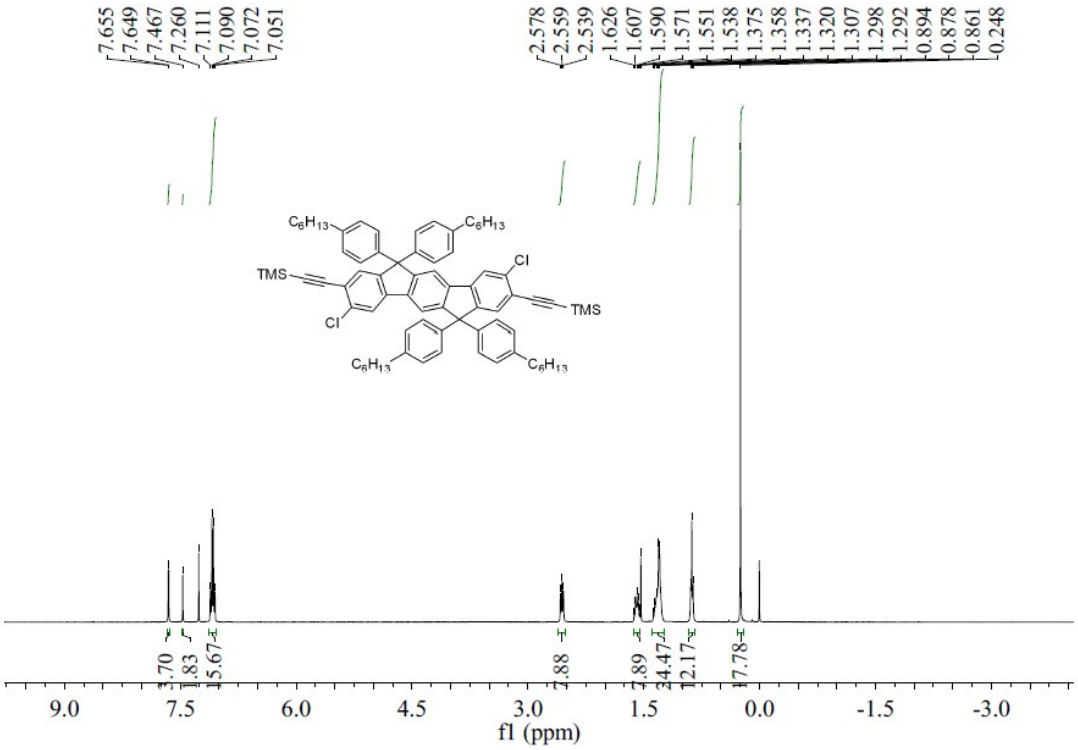

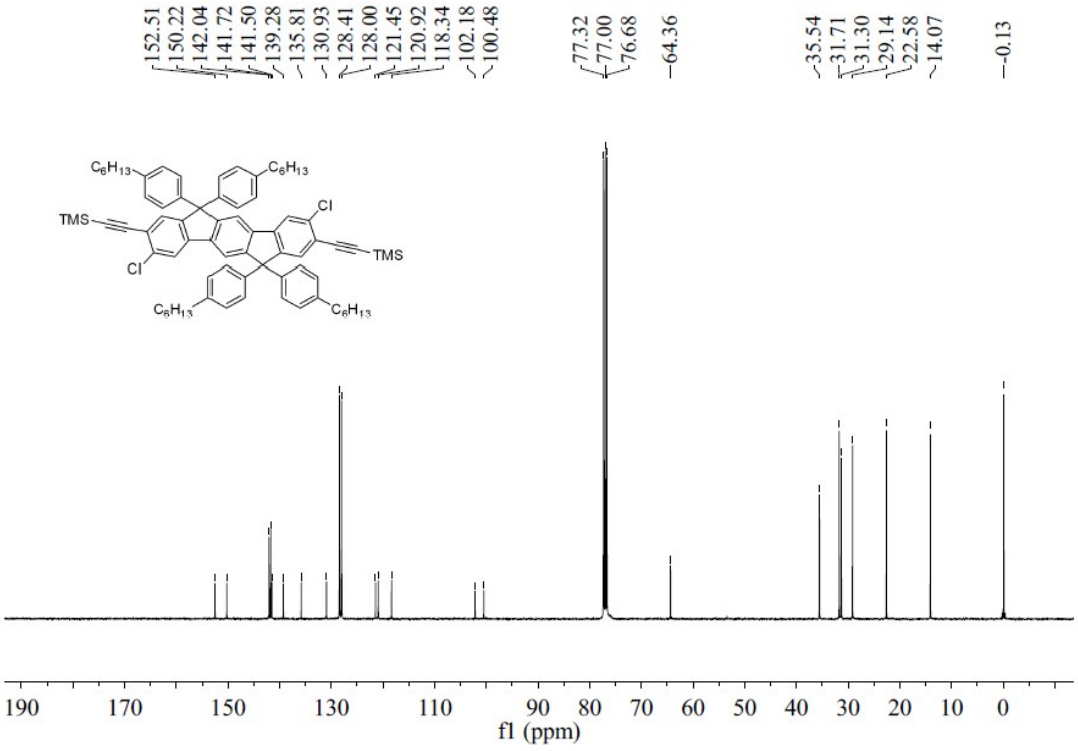

IDBT

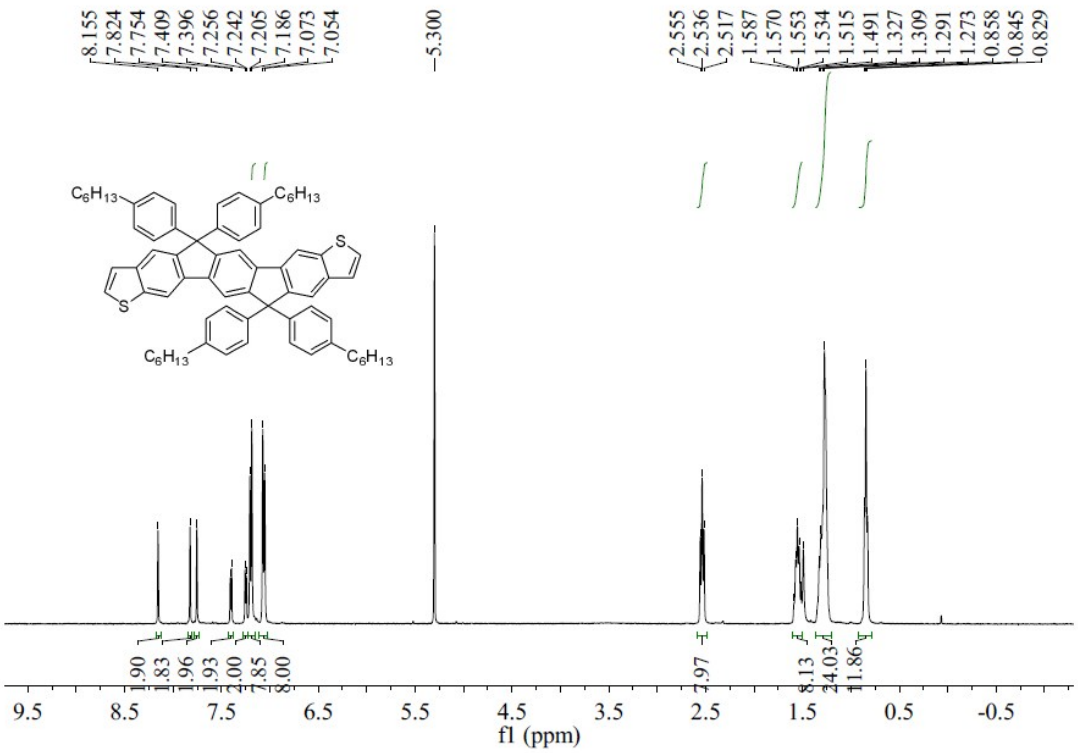
8.155
7.824
7.754
7.409
7.396
7.256
7.242
7.205
7.186
7.073
7.054
5.300
2.555
2.536
2.517
1.587
1.570
1.553
1.534
1.515
1.491
1.327
1.309
1.291
1.273
0.858
0.845
0.829
C6H13
S
1.90
1.83
1.96
1.93
2.00
7.85
8.00
7.97
8.13
24.03
11.86
9.5
8.5
7.5
6.5
5.5
4.5
3.5
2.5
1.5
0.5
-0.5
f1 (ppm)

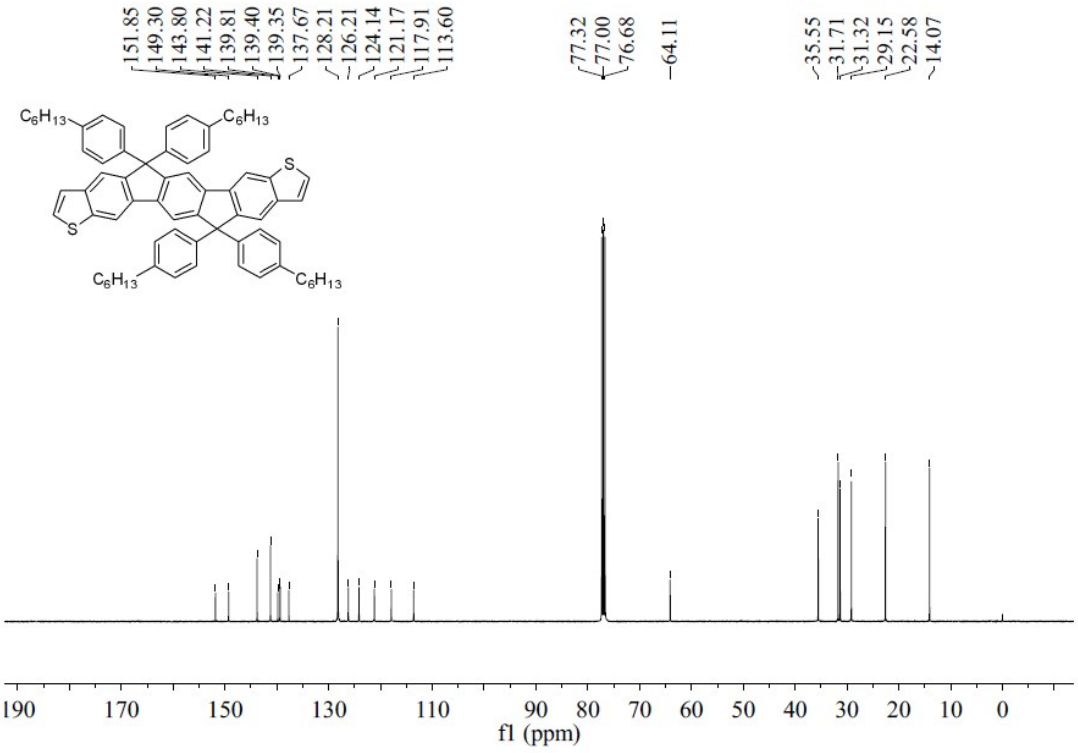
151.85
149.30
143.80
141.22
139.81
139.40
139.35
137.67
128.21
126.21
124.14
121.17
117.91
113.60
77.32
77.00
76.68
64.11
35.55
31.71
31.32
29.15
22.58
14.07
C6H13
S
190
170
150
130
110
90
80
70
60
50
40
30
20
10
0
f1 (ppm)

IDBT-CHO

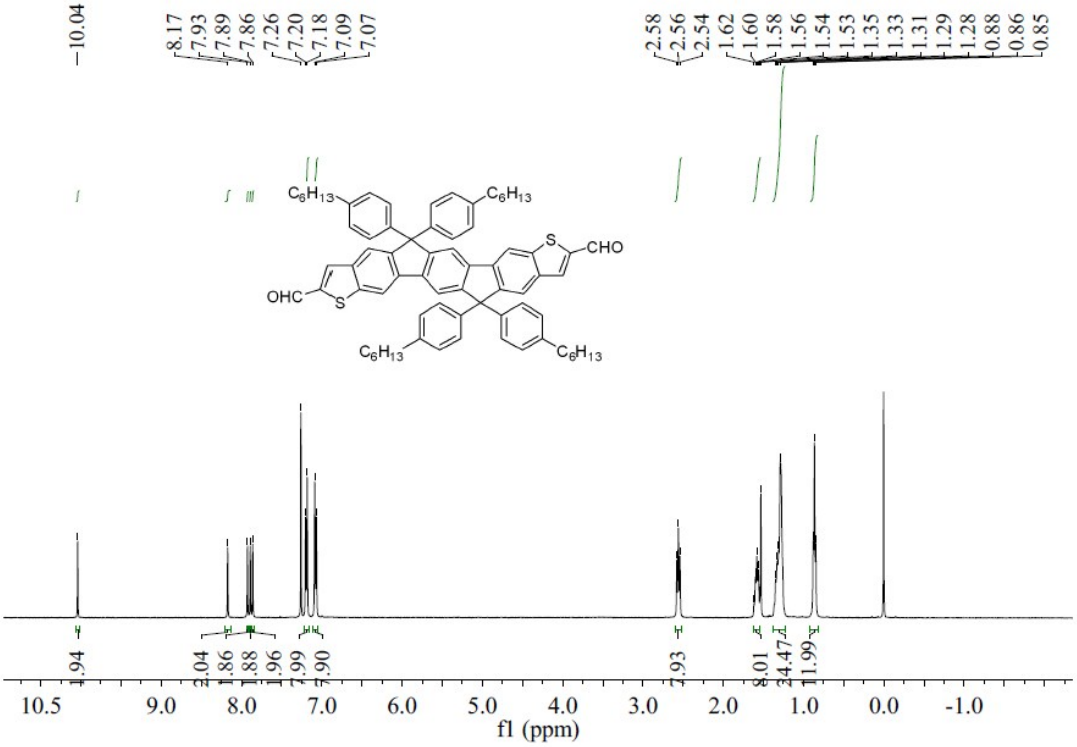
10.04
8.17
7.93
7.89
7.86
7.26
7.20
7.18
7.09
7.07
2.58
2.56
2.54
1.62
1.60
1.58
1.56
1.54
1.53
1.35
1.33
1.31
1.29
1.28
0.88
0.86
0.85
C6H13
C6H13
S
CHO
OHC
S
C6H13
C6H13
1.94
2.04
1.86
1.88
1.96
7.99
7.90
7.93
8.01
24.47
11.99
10.5
9.0
8.0
7.0
6.0
5.0
4.0
3.0
2.0
1.0
0.0
-1.0
f1 (ppm)

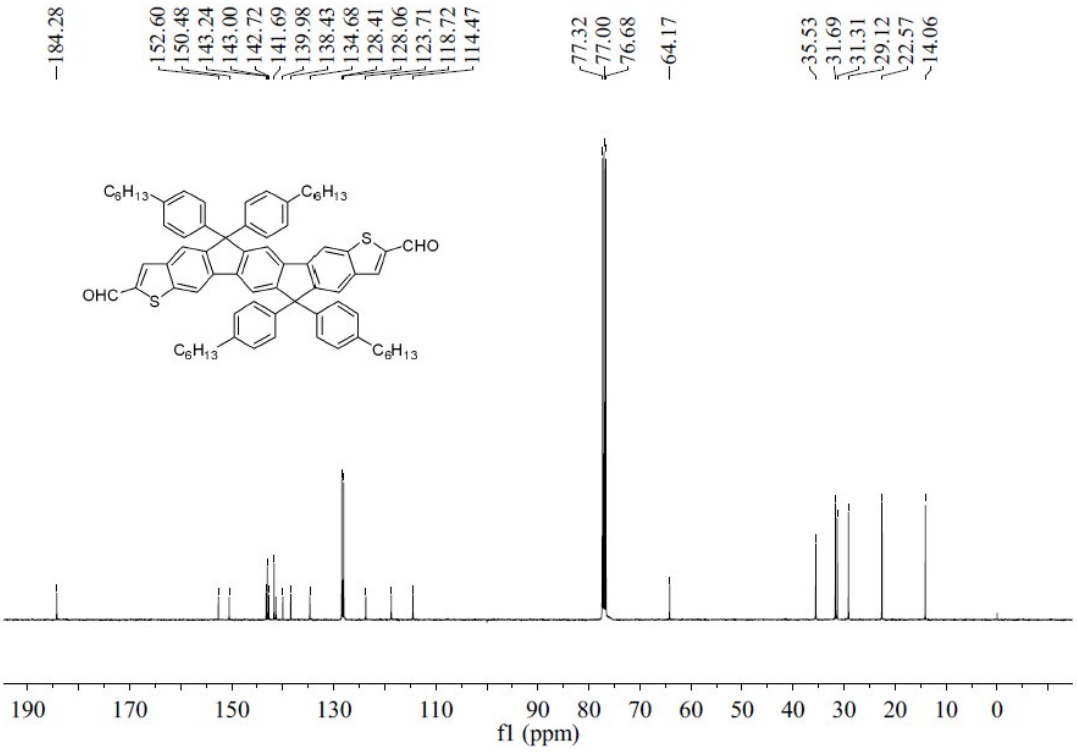
184.28
152.60
150.48
143.24
143.00
142.72
141.69
139.98
138.43
134.68
128.41
128.06
123.71
118.72
114.47
77.32
77.00
76.68
64.17
35.53
31.69
31.31
29.12
22.57
14.06
C6H13
C6H13
S
CHO
OHC
S
C6H13
C6H13
190
170
150
130
110
90
80
70
60
50
40
30
20
10
0
f1 (ppm)

NIDBT

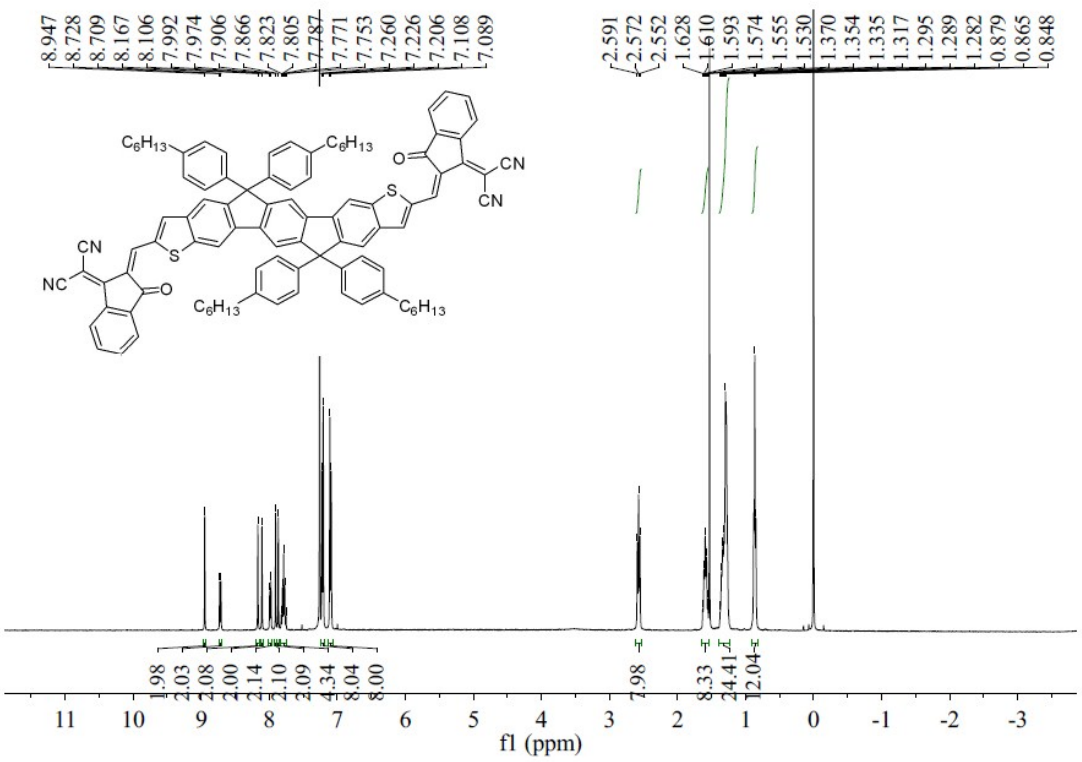
8.947
8.728
8.709
8.167
8.106
7.992
7.974
7.906
7.866
7.823
7.805
7.787
7.771
7.753
7.260
7.226
7.206
7.108
7.089
2.591
2.572
2.552
1.628
1.610
1.593
1.574
1.555
1.530
1.370
1.354
1.335
1.317
1.295
1.289
1.282
0.879
0.865
0.848
1.98
2.03
2.08
2.00
2.14
2.10
2.09
4.34
8.04
8.00
7.98
8.33
24.41
12.04
fl (ppm)

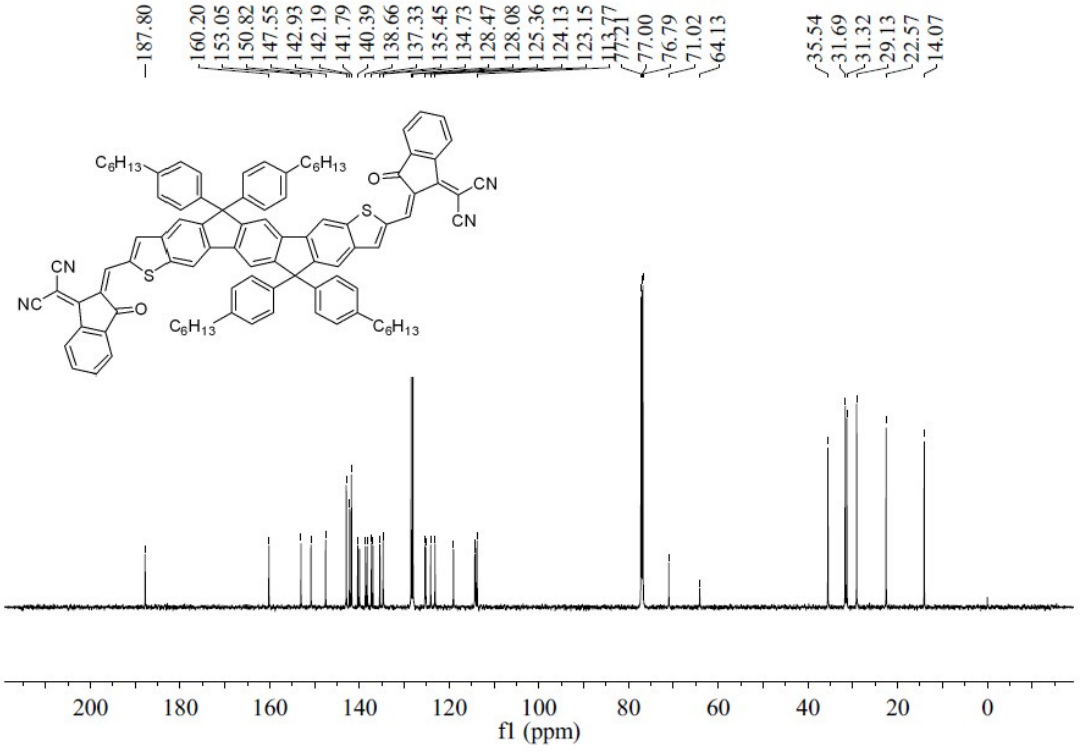
187.80
160.20
153.05
150.82
147.55
142.93
142.19
141.79
140.39
138.66
137.33
135.45
134.73
128.47
128.08
125.36
124.13
123.15
113.77
77.21
77.00
76.79
71.02
64.13
35.54
31.69
31.32
29.13
22.57
14.07
fl (ppm)